Hydrogeochemistry of intermittent alluvial aquifers controlling arsenic and fluoride contamination for corresponding influencing health risk assessment

Sandip Sampatrao Sathe (sandipsathe1425@gmail.com)
Indian Institute of Technology Guwahati
Chandan Mahanta
Indian Institute of Technology Guwahati
Senthilmurugan Subbiah
Indian Institute of Technology Guwahati

Research Article

Keywords: Arsenic, Hydro-geochemistry, Groundwater, water quality index, health risk assessment, Brahmaputra Flood Plain

Posted Date: March 18th, 2021

DOI: https://doi.org/10.21203/rs.3.rs-214557/v1

Hydrogeochemistry of intermittent alluvial aquifers controlling arsenic and fluoride contamination for corresponding influencing health risk assessment

Sandip S. Sathe[1,2*], Chandan Mahanta[1], Senthilmurugan Subbiah [2]

[1]Department of Civil Engineering, Indian Institute of Technology Guwahati, Guwahati, Assam 781039, India

[2]Departmemt of Chemical Engineering, Indian Institute of Technology Guwahati, Guwahati, Assam 781039, India

*Corresponding Author: Sandip S. Sathe

Email: s.sathe@iitg.ac.in

(+91- 8822301580)

Abstract

Identification and management of safe groundwater supply in a high *As* and F^- contaminated region is a major concern facing most of the developing countries worldwide. This study provides a comprehensive hydrogeochemistry result for a complex hydro-stratigraphy soil aquifer, which is bound between the Shillong plateau and Himalayan ranges in the North-Eastern region of India. In this study, distinct contaminated regions of *As* and F^- were identified in rainy (n=94) and winter (n=50) seasons groundwater samples. The maximum dissolved concentration of *As* was measured as 71 µg L^{-1} in rainy and 211 µg L^{-1} in winter season groundwater samples, whereas maximum F^- concentration was measured as 7 mg L^{-1} in rainy and 6 mg L^{-1} in winter season groundwater samples. Identified minerals saturation condition, weathering, and dissolution results of hydrogeochemistry were well corroborated with the Bivariate plot, Gibbs and Pourbaix diagrams. Results of health risk assessment showed that population of age below 18 years old are prone to carcinogenic diseases and symptoms of non-carcinogenic health risk due to daily consumption of *As* contaminated groundwater. Children of age below 18 years old, in total 39% (i.e. 6834) and 64% (i.e. 13937) were found more susceptible to arsenic ingestion effect. The male population was found prone to *As* cancer risk than the female population. Overall, this study provides a critical result about the cause of high *As* and F^- concentration in groundwater and health risk assessment, it provides a prime concern matter for the young generation which is at higher risk of *As* cancer.

Keywords: Arsenic; Hydro-geochemistry; Groundwater; water quality index, health risk assessment; Brahmaputra Flood Plain

1 Introduction

Shallow depth groundwater aquifers contaminated by arsenic (*As*) and fluoride (F) in alluvial aquifer is a major concern for endemic diseases of arsenicosis and fluorosis due to

daily water usage in most of the developing countries (Fendorf S 2010; Wen et al., 2013). Growing urban population and industrial development in South-Asian countries like India, China, Sri Lanka Bangladesh, Nepal, Vietnam, Bhutan, Pakistan etc. are primarily dependent on shallow aquifer groundwater for drinking, irrigation, domestic purposes (Mandal and Suzuki 2002; Nordstrom 2002; Schaefer et al., 2017). Alluvial groundwater aquifer (i.e. Holocene Age) of Brahmaputra river basin are known for severely affected by high dissolved concentration of *As* and F in the world (Enmark and Nordborg 2007; Goswami et al., 2014; Mukherjee et al., 2015; Mahanta et al., 2015; Mahanta et al., 2016; Kumar et al., 2016; Sathe et al., 2016; Sathe et al., 2018; Sathe and Mahanta 2019a; Sathe 2019b; Sathe et al., 2020). Elevated concentration of *As* (i.e. more than 10 µg L^{-1} as guided by WHO permissible limit for drinking water) in the groundwater has earlier reported by Singh 2004, subsequently other researchers have validated and checked different hypothesis for the cause of high *As* and F in Brahmaputra flood plain (Smedley and Kinniburgh 2002; Goswami et al., 2014; Mukherjee et al., 2015; Mahanta et al. 2015; Patel et al., 2017). Goswami et al., 2014 have conducted health study on Majuli river island of the Brahmaputra river, where they measured mean *As* concentration in urine, hair and nail samples of local people as 158 µg L^{-1}, 1223 µg L^{-1} and 2507 µg kg^{-1} respectively.

Indiscriminate use of Brahmaputra river and its tributaries like the Bharalu river as pathway for sewerage and industrial waste carrier has made the Brahmaputra river water unsafe for drinking and domestic usage in the Guwahati city. In early 1970s, demand for safe and sufficient water source have encourage people to use the shallow aquifer groundwater for daily usage (Mukherjee et al., 2007). Consequently, several water supply schemes such as roadside public hand pumps for limited families (i.e. around 50 family) and pipe water supply schemes for around 1000 families were installed by government organizations for the urban and village people (Enmark and Nordborg 2007; Mahanta et al. 2015).

71 Drinking contaminated groundwater with high dissolved concentration of *As* have resulted
72 in severe chronic health effects, such as hyperpigmentation, keratosis, abnormalities since birth
73 and miscarriages, circulatory, neurological and behavioural disorders, premature hair greying,
74 respiratory complications, etc. and ultimately death due to *As* cancer (WHO 1993; Gebel 2000;
75 National Academy Press 2001). High *As* concentration in groundwater reported from
76 Brahmaputra flood plain is 606 µg L^{-1} (Mahanta et al., 2015) whereas in alluvial aquifer sand
77 it was measured as 61 µg kg^{-1} (Sathe and Mahanta 2019a). Concentration of *As* (up to 0.22 mg
78 kg^{-1}) in phosphate fertilizers were reported as a major anthropogenic source near agricultural
79 land.

80 Population affected by fluorosis are observed mainly form tropical countries like India,
81 China, Japan, Sri Lanka, Pakistan, Turkey, Korea, Italy, Brazil (Srinivasa Rao,1997; Brindha
82 et al., 2011). Symptoms of high F^- concentration groundwater consumption observed are bone
83 fluorosis and crippling bone, mostly found in human aged below 10 years due to prolonged
84 exposure to high F^- concentrations (Yadav et al. 2019). The toxic effect of F^- depends on age,
85 duration and immune system of person (Amalraj and Pius 2013). The other harmful effects
86 reported due to high F^- ingestion are a decrease in blood cells, osteoporosis, genetic damage
87 decrease thyroid function, mental retardation, hypertension, depression, impairment of nervous
88 system, premature aging, cancer and renal disease etc. (Hillier et al. 1996; Hurtado and
89 Tiemann 2000; Susheela et al. 2005; Xiong et al. 2007; Valdez-Jiménez et al. 2011; Sun et al.
90 2013; Jiang et al. 2019). Daily intake of F^- within the permissible limit is beneficial to health
91 and it protect from decaying of tooth from enamel to the tooth, also it helps in formation of
92 new bones (Adimalla and Venkatayogi 2017; Dehbandi et al. 2018). The major concern for
93 safe drinking water to authorities of developed countries is to maintain the desirable
94 concentration of F^- in drinking water (Jones et al. 2005; Petersen and Lennon 2004; Podgorny
95 and McLaren 2015).

In different regions of Brahmaputra flood plain, broad consensus was *As* mobilized into shallow aquifer groundwater is desorption and reductive dissolution of Fe oxy/hydroxide minerals and groundwater fluctuation (Smedley and Kinniburgh 2002; Mahanta et al. 2015; Sathe et al. 2019a). Few studies have presented the results on mobilization mechanisms and mitigation strategies for the groundwater *As* and F^- contamination problem in Brahmaputra flood plain (van Geen et al., 2008a; van Geen et al., 2008b; Mukherjee et al., 2015; Sathe et al., 2015). Brindha et al. (2011) have reported that dissolved fluoride concentration in groundwater may increases due to evaporation groundwater from the shallow aquifer may be affected by lowering of groundwater table in summer season in India. Groundwater table in Brahmaputra flood plain found at a depth of 5 to 10m from ground surface and groundwater table fluctuation was observed at in between 3 to 5m (Mahanta et al., 2015; Sathe and Mahanta 2019). Such long-time residual time of groundwater with the aquifer material favour for the soil-water interaction and dissolute the fluoride in different groundwater pH conditions. Publication on health risk assessment on this area was vague and less studies have reported on the risk of consumption of groundwater and total people are at the risk of fluorosis in Brahmaputra flood plain.

The detailed mineralogical studies by XRD, morphological studies, and saturation indices (SI) have reported that the primary *As* and F bearing minerals were found to be the cause for high concentration in the Brahmaputra flood plain (Sathe et al., 2018; Sathe and Mahanta 2019a). The statistical analysis, Pourbaix diagram, Gibbs plot, and minerals saturation indices were helped to identify geochemical mechanisms and harmful metal species prevailing in the groundwater samples. Groundwater quality index study further assisted to identify appropriateness for various usage such as drinking, agriculture and industry (Kamboj & Kamboj 2019).

120 The carcinogenic health risk assessment provides a probable number of peoples who are
121 at the risk of ingestion and dermal effects of *As* contaminated groundwater sources (USEPA,
122 2012; Singh and Ghosh 2012). Table 1 shows concentration of *As* and F^- in groundwater and
123 river water measured in different countries and methods adopted for health risk assessment.
124 Few studies have conducted on health survey and measured concentration in the human body
125 for the north eastern states of India (Goswami et al., 2014). Understanding of spatial
126 distribution of chemical species by ordinary kriging method provides are occurring health risk
127 in the region and concentration variation pattern in the study area. The contour gradient of
128 kriging method helps to understand the direction of groundwater flow and predict future
129 contaminated region in the study area (Sathe and Mahanta 2019a). Schuh et al. (1997) found
130 that increasing trends in the groundwater aquifer for a particular solute were mainly caused by
131 recharge or infiltration from surface water bodies and partially controlled by anthropogenic
132 activities such as heavy pumping by irrigation well and community water supply wells in that
133 study area. Mukherjee et al., 2007 in West Bengal region and Sathe and Mahanta 2019a study
134 in Brahmaputra flood plain have observed that depth wise distribution of dissolved *As*
135 concentration in alluvial aquifers can be influenced by heavy groundwater pumping from the
136 deeper aquifer.

137 In north-eastern flood plain region of India mainly the Brahmaputra flood plain (Assam),
138 studies were focused on the identification of *As* and F^- sources, mobilization mechanisms, and
139 severely affected regions were reported. This study was aimed to find 1) suitability of
140 groundwater usage determined by water quality index, 2) identify primary and secondary *As*
141 and F^- minerals in the alluvial aquifer, 3) carcinogenic health risk assessment and 4) understand
142 the concentration gradient, delineate safe aquifer and low risk region for drinking water.

2 Study area

North-Eastern region of India mainly comprises eight states. The Guwahati city of Assam state has vital importance in terms of its industrial growth, agricultural fertile land and road connectivity. The study area is situated between a longitude of E 91.4666° to E 91.8868° and latitude N 26.2061° to N 26.0520° on the southern part of state Assam, it covers an area of 328 km² (Figure 1). Total population of city is 1,116,267 and population density as 3,400/km^2 in Guwahati city (Population of Guwahati 2020). Guwahati city is growing from the foothills of the Shillong plateau. Outskirts of Guwahati city is occupied by industrial areas, government offices, colleges, schools, and the central part is densely populated with a residential building and shopping malls.

Bharalu River is one of the tributaries of Brahmaputra river, it originates in the Khasi Hills of Meghalaya flows through the centre of the Guwahati city and confluence with the Brahmaputra river on the northern side of the city (Figure 1). This tributary river has vital importance in terms of water and sewage water carry from the city. Guwahati city receives an annual rainfall of 1,752 mm (IMD Guwahati 2020). Most of the people in city uses groundwater as a source for drinking and domestic purposes in the city. The groundwater supply tubes are usually installed at a depth of 100 ft. to 150 ft. whereas government tube wells are usually installed below 250 ft. to 1000 ft. depth.

3 Materials and method

3.1 Groundwater sampling

For rainy season, groundwater samples were collected in such a way that it covers the entire Guwahati city, whereas in the winter season, high dissolved concentration of *As* and F^- areas were mainly targeted to understand the concentration variation in different seasons. For the rainy season, 94 groundwater sample and in the winter season, 50 groundwater samples

were collected in a month of November 2019 and in January 2020. The water samples were deliberately collected from government and private bore well sources, obligatory information for each groundwater sources (viz. private wells, hand tube wells and open well) such as screen depth, water table depth, discharge rate, installation year, number of people depend on it, water-related health issue reported since installation, and GPS coordinates (Garmin Montana 610) were collected during sampling. The stagnant groundwater (i.e. partially oxidized) was expelled out by continuous pumping for 10 minutes before sample collection from each tube wells and stored in 250 mL capacity high-density polyethylene bottles (Tarson, India). Groundwater were stored in two different sets, for cation analysis samples was acidified by adding few drops of HNO_3 and made its pH below 2 (1% v/v, Suprapur, Merck) and another set of non-acidified groundwater sample was collected for anion analysis. Precaution was taken during groundwater sampling and bottles filled by ensuring that there is no headspace left in the sampling bottles, bottles were stored in dark place and cold room.

3.2 Groundwater analysis

The time and temperature-dependent groundwater hydro-chemical parameters such as electrical conductivity (EC), dissolved oxygen (DO), pH, total dissolved solids (TDS), temperature (°C) and oxidation-reduction potential (ORP) were measured on-site during sampling using a multiparameter (YSI Inc. 550A, Sondes) water testing kit. Ion chromatography (M/s Metrohm, Switzerland) instrument was used to measure the selective cation and anion concentration in groundwater samples. For the analysis, Metrosep C2-250, 4×250 mm column was used and operated at 20 °C. Before every groundwater sample analysis, samples were filtered through a 0.2 μm filter (Whatman, 6872-2502 GD/X 25 mm Syringe Filter, PVDF filtration medium). A mobile phase of 1 litre was prepared by adding 100 mL of pyridine dicarboxylic acid and 1.7 mL of 1M HNO_3 solution in 1 litre of volumetric flask. The mobile phase solution prepared for IC instrument analysis was maintained at 1 mL min^{-1} flow

192 rate and pressure 80 MPa applied during analysis. The instrument was calibrated before
193 analysis using multielement Ion Chromatography anion and cation standard solution (M/s
194 Merck).

195 Arsenic concentration in groundwater samples were determined by a hydride generation
196 atomic absorption spectrophotometer (HG-AAS, VGA-77 detection limit <1 μgL^{-1})
197 instrument. The total concentration of iron and manganese was determined by a graphite
198 furnace atomic absorption spectrophotometer (GF-AAS, GTA-120, Varian, SpectrAA-55).
199 The minimum concentration detection limit for Fe was 1.5 $\mu g\ L^{-1}$ and for Mn it was 1.0 $\mu g\ L^{-1}$
200 (Sathe et al., 2018).

201 **3.3 Speciation modelling**

202 The minerals saturation Indices (SI) for predominant minerals were calculated using
203 Visual MINTEQ 3.1 software using groundwater hydrogeochemistry results in following Eq.
204 (1) Gustafsson, 2014):

205 $$Saturation\ Indices\left(SI\right) = \log(IAP \times KT) \ldots \text{ equation (1)}$$

206 whereas ion activity product is abbreviated as 'IAP' and 'KT' represents at ambient
207 temperature, equilibrium solubility constant for particular mineral. Thermodynamic database
208 present in software (i.e. thermo. vdb) was used for the determination of respective minerals
209 'SI' values. The 'SI' for minerals possessing positive, zero, and negative values have suggested
210 that these minerals are thermodynamically supersaturated, equilibrium, and unsaturated
211 respectively. Redox coupling was assigned mainly for As^{+3} / As^{+5}, Fe^{+2} / Fe^{+3} and Mn^{+2} / Mn^{+3}
212 metal species.

213 **3.4 Ordinary kriging**

214 Kriging is a stochastic method commonly applied for spatial data interpolation which
215 provide the possible values of particular solute at unsampled sites. For present study, to
216 understand the spatial concentration variation of Mn, F^-, Fe, and *As* in different depths of
217 aquifer, ordinary kriging method with combination of variogram method were applied. In this
218 method, the measured surrounding values were used directly in the empirical mathematical
219 formulas, which provide intermittent spatial data in terms of contour values for the delineated
220 study area. The ordinary kriging method assumes the constant mean as unknown, this method
221 is more relevant when there is a spatial correlation in distance and directional bias in the
222 analysed data. Ordinary kriging method often practiced in geology and agricultural department
223 for understanding variability of soil strata (Oliver and Webster 1990). The optimum values for
224 range, sill, nugget, azimuth-angle, contribution, dip-angle, and plunge-angle were used in such
225 a way that it can accommodate minimum and maximum distance sample location for empirical
226 semi-variogram model of Spherical, Exponential, Gaussian analysis. The applied empirical
227 semi-variogram model provides an information on the spatial autocorrelation of datasets.

228 Groundwater modelling software i.e. GMS 10.2 was used by considering anisotropy of
229 for spatial and vertical distribution (i.e. three-dimensional) of aquifer material for *As*, Fe, F^-,
230 and Mn distribution analysis. In kriging method, values in between were determined by
231 assuming that over a region's values varied continuously (Deutsch and Journel, 1992). The
232 ordinary kriging method solves the following equations;

233 $$\gamma(\bar{\chi},\bar{y}) = \frac{1}{2N} \times \sum (Z(\bar{\chi}) - Z(\bar{y}))^2 \ldots \text{equation (2)}$$

234 Where, variables at point $\bar{x}$ and $\bar{y}$ are $Z(\bar{\chi})$ and $Z(\bar{y})$, and N is a number of data pairs.
235 Variogram in the form of $\gamma(h)$ which is based on the planar distance of 'h' between two points
236 $\bar{x}$ and $\bar{y}$. Following equation was used in ordinary kriging method:

237 $$Z(\bar{x}_o) = \sum_{i=1}^{N} \lambda_i \times Z(\bar{x}_i) \ldots \text{ equation (3)}$$

238 where the estimated and observed values at point $\bar{x}_o$ is $Z(\bar{x}_o)$ and at 'ith' point $\bar{\chi}_i$ is $Z(\bar{\chi}_i)$.

239 Observed value in the 'λ_i' point is the weight of $\bar{x}_i$ and 'N' is the total number of observed

240 points. Following semi-variogram models such as exponential, theoretical spherical, and

241 gaussian were used for the kriging method.

242 Spherical model;

243 $$\gamma(h) = C_o + C\left[1.5\left(\frac{h}{a}\right) - 0.5\left(\frac{h}{a}\right)^3\right] \quad h \le a \quad \ldots \text{ equation (4)}$$

244 $$\because C_o + C \quad h > a$$

245 Exponential model;

246 $$\gamma(h) = C_o + C\left[1 - \exp\left(-\frac{3h}{a}\right)\right] \ldots \text{ equation (5)}$$

247 Gaussian model;

248 $$\gamma(h) = C_o + C\left(1 - \exp\left[-\left(\frac{3h}{a}\right)^2\right]\right) \ldots \text{ equation (6)}$$

249 where 'C_O' is the nugget effect; 'C' is the sill; and 'a' is the range. The spatial data required

250 for semi-variogram models provided by theoretical semi-variogram model used in these

251 analyses.

252 **3.5 Weighted arithmetical water quality index (WQI)**

253 To classify the groundwater quality WQI method was followed. This a common method

254 usually used by hydrogeochemistry experts (Chauhan and Singh 2010; Chowdhury et al., 2012)

255 for the decision-making policy and followed WQI equation (Rown et al., 1972) for the

256 calculation:

$$WQI = \frac{\sum Q_i W_i}{\sum W_i} \ldots \text{ equation (7)}$$

For each parameter, using following equation a quality rating scale i.e. 'Q_i' was calculated

$$Q_i = 100 \times \left[\left(\frac{V_i - V_o}{S_i - V_o} \right) \right] \ldots \text{ equation (8)}$$

Where, estimated concentration is abbreviated as 'V_i' for 'i^{th}' parameter, is abbreviated as 'V_o' for pure water. The standard recommended value i.e. 'S_i' for 'i^{th}' parameter, ideal pure water is 'V_o' = 0 (except pH =7.0 and DO = 14.6 mg L^{-1})

The unit weight 'W_i' for each sample was calculated by using following equation:

$$W_i = \frac{K}{S_i} \ldots \text{ equation (9)}$$

Where, proportionality constant is abbreviated as 'K' and calculated using following equation:

$$K = \frac{1}{\sum \left(\frac{1}{S_i} \right)} \ldots \text{ equation (10)}$$

Obtained WQI values were categorized into five grades (i.e. A to E) and rated for each groundwater samples. The WQI values laid in between 0 to 25 was categorized in "Grade – A" and rated as "Excellent water quality" which suggest that it is safe for drinking purposes. The WQI value between 26 to 50 is rated as "Good water quality" and graded in the "B" category. The third category is "Grade-C" and rated as "Poor water quality" for WQI values laid between 51 to 75. The "Grade- D" category water rated as "Very poor water quality" for WQI values laid between 76 to 100. The WQI values above 100 is graded as "E" and rated as "Unsuitable for drinking purpose".

3.6 Carcinogenic health risk assessment (CH_A)

Carcinogenic health risk assessment posed by drinking groundwater with high dissolved concentration of *As* on present population was assessed by following USEPA 2004 guideline. Mainly ingestion of *As* and risk assessment for dermal was evaluated by using the following empirical equations (11) & (12):

$$ADD_{Ingestion} = \frac{(C_w \times IR \times EF \times ED)}{(B_w \times AT)} \ldots \text{equation (11)}$$

$$ADD_{Dermal} = \frac{(SA \times EF \times C_w \times K_p \times ED \times ET \times CF)}{(AT \times BW)} \ldots \text{equation (12)}$$

Where, heavy metals average concentration in groundwater samples is 'C_W' (µg L^{-1}); 'IR', ingestion rate (L day^{-1}) the adopted IR values for this study was 2.0 L day^{-1} and 0.64 L day^{-1} for adults and children (Xiao et al., 2019), exposure frequency is abbreviated as 'EF' (days $year^{-1}$) and 350 days $year^{-1}$ values used for the calculation (USEPA, 2004), exposure duration is abbreviated as 'ED', and 70 years and 6 years maximum value was adopted for the adults and children population respectively. Average body weight IS abbreviated as 'B_W' for the calculation, 60 kg and 15 kg maximum weight was considered for adults and children population (Njugunaet al., 2019; Saleem et al., 2019). The average exposure time is abbreviated as 'AT' and for the above calculation 70 years and 6 years was adopted for adults and children populations. Surface area of the skin is abbreviated as 'SA' whereas, 6,600 cm^2 and 18,000 cm^2 values used for children and adult's population. Dermal permeability coefficient is abbreviated as 'K_p' and for calculation 0.001 cm h^{-1} value adopted for *As* contaminant (EPA 2004). 'ET' abbreviated for exposure time, for bathing and shower, 0.25 h day^{-1} 'ET' value was adopted for the calculation. 'CF' is a unit conversion factor, 0.001 L cm^{-3} (USEPA, 2004). According to 'ADD $_{ingestion}$' and ADD $_{Dermal}$' calculation, the values below one (i.e. <1) suggested that these groundwaters sources are safe for drinking water purposes but values above one (i.e. >1) indicate that these groundwater sources are unsafe for drinking purposes

and particular the population is at the risk of early carcinogenic effect due to drinking of *As* contained groundwater (Njuguna et al., 2019).

4 Results and Discussion

4.1 Groundwater hydrogeochemistry

Groundwater quality monitoring for carcinogenic and toxic chemicals at different depth of aquifers and sources was meticulously studied in this analysis. The results of temperature and time sensitive parameters such as pH, DO and ORP for rainy season groundwater samples depict that the acidic to alkaline nature by pH (5.9 to 8.9) values, ORP results showed low (i.e.-359 mV) to high (i.e. 503 mV) reducing condition and DO results (i.e. 0.9 mg L^{-1} to 7.8 mg L^{-1}) in groundwater samples. Similarly, in winter season pH (viz. 6.3 to 9.3) shows near neutral to alkaline and hard water condition, ORP showed strong reducing (viz. - 498 mV to 189 mV) condition prevailing in groundwater aquifer. A common problem identified during personal interaction with the consumers was white colour scaling on inside of cooking utensils, encrustations in water supply structure and inside of water supply pipe lines.

The results of cation and anion analysis provides a vital information to assess the health of groundwater consumers and identify possible solution required for the study area. Groundwater temperature, DO are an important parameter which provide signs of present physicochemical process and biological activity prevailing in groundwater aquifers (Ali, Islam, & Rahman, 2016). Comparatively, in the winter season, high concentration of NO_3^- as 25.2± 3.7 mg L^{-1} (i.e. maximum ± S.D) was found (Table 2a and 2b), which indicates excess use of pesticides on adjoining agricultural land and it consequently infiltrate into shallow depth groundwater aquafer. These anthropogenic sources of *As* and F^- chemicals in groundwater aquifer provide a favourable condition for microbial mineralization. The measured high concentration of SO_4^{-2} (82.9 ± 16.2 mg L^{-1}) and Cl^- (105 ±23.8 mg L^{-1}) in winter season

groundwater samples suggest the secondary salinity source is a cause for high concentration. Compared to rainy season, the winter season groundwater results showed high concentration of HCO_3^- (418 ± 63 mg L^{-1}) which indicates active weathering process of carbonaceous minerals in shallow depth aquifer. High concentration of dissolved fluoride (i.e.7.3 ± 1.3 mg L^{-1}) was observed in the rainy season groundwater samples than winter season (i.e. 6.1 ± 1.3 mg L^{-1}) samples, which indicates favourable aquifer conditions for a geogenic source of fluoride bearing minerals (viz. fluorite, mica, biotite) (Chaurasia et al. 2007). The anionic analysis for the rainy season samples showed concentration wise abundance as $HCO_3^- > Cl^- > SO_4^{-2} > F^- > NO_3^-$ similarly, in winter season it is measured as $HCO_3^- > Cl^- > SO_4^{-2} > NO_3^- > F^-$ for study area groundwater samples.

Dominant Na^+ cation concentration was measured in the rainy season groundwater sample results. The descending cation concentration order was found as $Ca^{+2} > K^+ > Mg^{+2}$ whereas similar concentration trend was observed in winter season groundwater results, except for few samples Mg^{+2} concentration was observed high as 12038 mg L^{-1}, 2661 mg L^{-1} and 3912 mg L^{-1}. There was significant concentration variation in the winter season groundwater analysis results, where more than 50% decrease in concentration of Fe was measured, which indicates that study area aquifers are prone to high aquifer flushing and dilution (Table 2a, 2b). In both seasonal groundwater sample analysis results, high dissolved Na^+ concentration has indicated that alumino-silicate and/or sodium-silicate minerals weathering or dissolution process was the cause for high concentration in the study area aquifer. Similarly, high concentration of Ca^{+2} indicates weathering of carbonate mineral such as gypsum, plagioclase and feldspar minerals which was a second dominant process prevailing in the groundwater aquifer (Sathe and Mahanta., 2019a). The high concentration of Na^+, Ca^{+2}, K^+ and Mg^{+2} in groundwater analysis also indicates the influence of high cation exchange mechanism, evaporation, infiltration of

surface water from sewage and agriculture land, and poor drainage system in study area (Kumar et al., 2006).

4.2 Hydrogeochemistry of arsenic and fluoride

The arsenic concentrations were measured between bdl to 71.3 ± 13.8 µg L^{-1} in the rainy season groundwater samples whereas for toxic arsenite [i.e. *As* (III)] species as it was measured in between bdl to 9.7 ± 2.4 µg L^{-1} in rainy season sample and comparatively low toxic arsenate [i.e. *As* (V)] species measured between bdl to 212 ± 32.8 µg L^{-1} in winter season groundwater samples. High concentration values of *As* in winter season samples was significantly correlated with on-site measured ORP value results which suggests that reducing groundwater aquifer favourable for dissolved arsenic concentration in the study area. Similarly, more than WHO drinking water permissible limit for Fe was measured as 24 ± 3.3 mg L^{-1} in rainy season samples and for Mn it was measured as 0.9 ± 0.2 mg L^{-1} and in winter season 0.3 ± 0.1 mg L^{-1} support reductive dissolution mechanism prevailing in study area aquifer. Studies have reported that high manganese in groundwater can causes low intelligence quotient in children (Khan et al., 2012). High concentration of Fe and Mn measured in rainy season samples suggested that the aquifer is under reducing condition and favourable for reductive dissolution mechanism of iron oxy/hydroxide minerals in groundwater aquifer.

The hydrogeochemical process such as weathering and dissolution are the dominant mechanism for high dissolved fluoride in groundwater aquifer (Saxena and Ahmed, 2003; Adimalla and Venkatayogi, 2017). Dissolution of fluorine in acidic conditions were observed due to complexes of aluminum difluoride (AlF_2^+) and di-fluoroaluminum (AlF_2) in groundwater (Wenzel and Blum 1992). Wenzel and Blum (1992) study have inferred that fluorine solubility increases above pH> 6.5 due to repulsion of negatively charged surfaces such as clay present in groundwater bearing aquifer. Therefore, the risk of groundwater is high

372 at strong acidic (pH < 6) as well as high alkaline (pH > 6.5) groundwater condition (Wenzel
373 and Blum 1992).

374 Dissolved form of fluoride is vulnerable to the ion exchange process, with hydroxyl anion
375 because of almost equal ionic radius of OH^- (i.e. 1.40 A°) and F^- (i.e. 1.36 A°). Furthermore,
376 dissolution and weathering of fluoride containing minerals such as muscovite, biotite,
377 hornblende and amphibole are favourable to sodium bicarbonate dominant facies in the
378 groundwater aquifer (Handa 1975). In piper plot predominant hydrogeochemical facies found
379 are Ca^{2+}– Na^+– HCO_3^- and Ca^{2+}– HCO_3^- suggested that the groundwater of the study area is
380 favourable to fluoride bearing minerals dissolution and allow precipitation of Ca^{2+} and
381 CO_3^{2-} ions in aquifer. Higher concentration of HCO_3^-, Na^+ and pH favours for the release of F
382 in in groundwater aquifer (Kumar et al., 2017). Ion exchange process between Na^+ and Ca^+ in
383 weathered aquifer zone increases F^- concentration whereas it decreases with increasing Ca^+
384 concentration due to precipitation of CaF_2 in groundwater aquifer. Thus, co-occurrence of *As*
385 and F^- in groundwater mainly due to desorption from Fe (hydro)-oxides and CaF_2 bearing
386 minerals surfaces (Gomez et al., 2009).

387 **4.3 Statistical analysis and mineral saturation indices**

388 The primary groundwater analysis results have depicted that groundwater aquifer of
389 depth 200 ft. to 500 ft. can yield *As* (Figure 2a) and F^- (Figure 2b) safe groundwater. The
390 statistical analysis by Pearson correlation method showed positive correlation value as $\rho = 0.6$
391 between dissolved concentration of *As* vs Fe for rainy season samples. It suggests significant
392 affinity with dissolved concentration values for each other. In winter season, insignificant
393 Pearson correlation values such as $\rho = 0.04$ was observed between *As* vs. Fe (Figure 2c), it
394 suggests that aquifers of the study area are highly susceptible for flushing capacity and
395 vulnerable to surface water infiltration. Other Pearson correlation analysis in both the season
396 groundwater samples for *As* with HCO_3^-, SO_4^{-2} and Mn showed (Figure 2d, 2e and 2f),

insignificant correlation values, which suggests that groundwater aquifer have high hydraulic conductivity and have less residential time.

Hydrogeochemical facies were identified in Piper plot using GW chart software (Current Version 1.30.0) developed by USGS (Piper 1944). Piper plot includes three distinct diagrams which consists of two triangles, one for cation (i.e. Ca^{+2}, Mg^{+2}, K^{+} and Na^{+}) and another for anion (i.e. HCO_3^{-}, SO_4^{-2}, Cl^{-} and CO_3^{-}) whereas one diamond-shape diagram plot shows combine cation and anion facies (Sathe et al., 2018). The results of piper plot showed three dominant hydrogeochemical facies in rainy season, such as 1) Ca^{+2} – HCO_3^{-} 2) Ca^{+2} – Na^{+} – HCO_3^{-} 3) Na^{+}–SO_4^{-2}–Ca^{+2} – HCO_3^{-} whereas, in winter season major two hydrogeochemical facies mainly 1) Ca^{+2} – HCO_3^{-} and 2) Ca^{+2}–Na^{+}–HCO_3^{-} were identified in groundwater samples (Figure 3). These distinct hydrogeochemical facies, indicates alkali mineral dissolution and causes alkaline and acidic nature of rainy and winter season groundwater. The high Na^{+} concentration coupled with low Ca^{+2} concentration suggests that the cause of ion exchange process and precipitation of CaF_2 in the groundwater aquifer. It suggests that the measured low concentration of F^{-} in respective wells groundwater samples are safe for drinking purposes in the study area. Results of hydrogeochemical facies observed in Piper plot were well supported with the previous studies results of Brahmapootra flood plain (Enmark and Nordborg 2007; Mahanta et al., 2015; Sathe et al., 2018).

Hydrogeochemical processes and mechanisms such as evaporation, weathering, and dissolution of minerals were identified using cation and anion concentration data in two-dimensional scatter plot for the study area. The sample concentration close to the line 1:1 in scatter plot of SO_4^{-2} + HCO_3^{-} versus Ca^{+2} + Mg^{+} (Figure 4a) indicates dissolution of minerals such as calcium and magnesium bearing gypsum, dolomite and calcite are the cause for high *As* and F^{-} concentration the groundwater aquifer (Cerling et al., 1989). Groundwater samples laid near to right side of the graph indicates that ion exchange process prevailing in the aquifer

samples due to excess dissolved concentration of SO_4^{-2} + HCO_3^- in groundwater (Fisher and Mulican 1997). Whereas, insignificant cation ion exchange process in groundwater samples was observed in excess concentration of Ca^{+2} + Mg^+ in samples, which are laid near to the left corner in the two-dimensional scatter plot (Cerling et al., 1989). Similarly, scatter plot of (Ca^{+2} + Mg^+) / HCO_3^- versus Cl^- indicates presence of Mg^+ and Ca^{+2} in samples. Ratio below 1 or around 0.5 indicates Ca^{+2} and Mg^+ concentration is solely added into groundwater by the dissolution and weathering of carbonates minerals also with accessory minerals such as pyroxenes and amphibole (Sami1992). Scatter plot results show that concentration of Ca^{+2} and Mg^+ is mainly controlled by dissolution and weathering of carbonate and amphibole minerals in the aquifer. The insignificant ion exchange process was observed in Ca^{+2} + Mg^+ versus Cl^- plot, its affinity with the dissolved concentration of Ca^{+2} + Mg^+ and salinity was observed in both season groundwater samples (Figure 4c).

Gibbs diagram often shows a relationship between lithological characteristics with the subsurface groundwater composition (Gibbs 1970). The Gibbs diagram distinctly divided into three distinct regions mainly precipitation, rock and evaporation. Most of the groundwater sample of rainy and winter season were laid in the rock domain, which suggests solid-liquid interaction process (i.e. weathering and dissolution process) of Na^+, K^+, and Ca^{2+} bearing minerals (Figure 4d).

4.4 Delineation of mineral saturation aquifers

The in-situ measured groundwater parameters such as pH and Eh were used to identify dominant *As*, F^-, Mn, and Fe species in the Pourbaix diagram (Figure 5a,5b,5c,5d). Mainly arsenate (As^{+3}) species (i.e. $H_XAsO_3^X$) higher dissolved concentration was found in rainy and winter season groundwater samples than arsenite (As^{+5}) species (i.e. $H_XAsO_4^X$) (Fgure 5a). The partial oxidizing groundwater condition were observed from Pourbaix diagram. The dominant fluoride species such as fluorite was observed in figure 5b. Similarly, the manganese bearing

447 dominant minerals rhodochrosite was observed in figure 5c and iron bearing minerals such as
448 siderite, ferrihydrite, and calcite species were identified in figure 5d from Pourbaix diagram.

449 Minerals saturation indices (SI) were determined using a hydrogeochemistry results of
450 *As*, Fe, F^- and Mn measured for rainy and winter season groundwater samples. The Visual
451 MINTEQ 3.1 software used for determination and identification of saturation values of primary
452 and secondary minerals. The inbuilt thermodynamic database and redox coupling species for
453 different metals were used before each sample analysis. The obtained negative SI values
454 signifies that these particular minerals are under unsaturated condition whereas positive SI
455 value signifies that respective minerals are at saturation condition in study area aquifer. The
456 reductive dissolution mechanism of iron oxy/hydroxide bearing mineral in the alluvium
457 aquifers of Brahmaputra flood plan for high dissolved concentration of *As* is broadly accepted
458 mechanism. Unsaturated condition for secondary arsenic minerals found mainly for arsenolite
459 (Avg. - 42 ± 4 & - 49 ± 4) and claudetite (Avg. - 42 ± 5 & - 49 ± 5) in rainy and winter season
460 groundwater samples respectively (Table 3). Therefore, these mineral results establish that the
461 source of dissolved *As* in groundwater aquifer is dissolution of secondary minerals. Saturated
462 iron-bearing minerals such as goethite (Avg. 6 ± 7 & 7 ± 1), ferrihydrite (Avg. 4 ± 49 & 5 ±
463 1), and hematite (Avg. 15 ± 12 & 17 ± 1) were found in rainy and winter season groundwater
464 samples. Saturation of these minerals in the aquifer sediment indicates that adsorption of *As*
465 species on the surface of these Fe bearing mineral and primary cause for low dissolved *As*
466 concentration in the *As* safe aquifer regions. In some regions mainly, siderite (Avg. -2 ± 5 & 0
467 ± 1) and vivianite (Avg. -2 ± 17 & -2 ± 9) were found in unsaturated conditions (Table 3),
468 supports the theory of desorption mechanism from iron oxy/hydroxide minerals (Smedley and
469 Kinniburgh 2002). These regions indicate aquifer are highly susceptible for surface water
470 infiltration and flushing ability. The prolonged groundwater trapped in the complex aquifer
471 strata, consequently cause for saturated Fe bearing minerals near Brahmaputra flood plain.

The unsaturated condition of fluorite mineral both seasons was observed as -38 to 0, have suggested that fluorite mineral is more soluble in alkaline groundwater condition than other F^- bearing minerals (Apambire et al., 1997; Farooqi 2015). In acidic groundwater condition, dissolution of minerals like amphiboles, micas and apatite is more favourable than fluorite mineral (Farooqi, 2015). The groundwater aquifer were observed rich in biotite and amphibole minerals, it is an indirect indication for the high F concentration in groundwater, beacsue fluorine substitutes a hydroxyl group from the biotite and amphiboles minerals (Edmunds and Smedley, 1996).

The bivariate plot results support the finding of hydrogeochemistry and Pourbaix diagram results (Figure 6). Unsaturated Fe bearing minerals were observed as hematite, goethite and ferrihydrite in rainy season (Figure 6a, 6c, 6e) whereas saturated minerals condition was observed in winter season for hematite, goethite and ferrihydrite mineral (Figure 6a, 6c, 6e) which was the cause for low dissolved concentration in winter season groundwater samples. In 2D bivariant plot, unsaturated mineral condition was found even at increased dissolved concentration of *As* (viz. arsenolite and claudetite) and F^- (viz. fluorite) bearing minerals in both season samples (Figure 6b, 6d, 6f).

Table 3 shows predominant *As*, Fe, Mn, and F^- bearing minerals saturation index in respect of rainy and winter season groundwater samples. The presence of secondary minerals suggest that the groundwater aquifers conditions are favourable for dissolution of primary *As* bearing minerals and convert into secondary minerals, which was the cause for high *As* dissolved concentration in the study area. The selective minerals saturation indices values were found for Fe bearing minerals such as goethite, rhodochrosite, siderite, ferrihydrite, hematite, and vivianite minerals in rainy and winter season groundwater samples (Table 3). The zero saturation indices value for Fe minerals indicates that these minerals are at stable conditions. The results of low *As* concentration with negative saturation indices values near the foothill of

497 Meghalaya state and Brahmaputra river region indicates that dissolved concentration in
498 groundwater aquifer is controlled by adsorption and desorption mechanism by Fe-hydroxide
499 minerals (Smedley and Kinniburgh 2002). Similarly, unsaturated (i.e. -38) and stable (i.e.0)
500 mineral condition for fluorite mineral suggests the primary source of F^- in groundwater aquifer.
501 High F^- concentration in groundwater and stable mineral were observed near Meghalaya state
502 foothill, which were further carried down by the surface water bodies (Table 3).

503 **4.5 Groundwater pollution assessment**

504 The groundwater quality index analysis deciphers the applicability of groundwater in
505 irrigation, domestic and drinking purposes. The groundwater quality index was classified into
506 five different categories, each signifies its usage for drinking purpose and daily usage. Total
507 48% (i.e. 45 samples) and 94% (i.e. 47 samples) of rainy and winter seasons groundwater
508 samples respectively, were found safe for drinking water usage (Table 4). It indicates
509 groundwater bearing aquifers are highly susceptible for surface water infiltration and dilute the
510 dissolved *As* and F^- groundwater concentration.

511 Based on groundwater hydrogeochemistry results a health risk assessment analysis was
512 carried out. The causes of primary symptoms and chronic diseases such as arsenical skin lesions
513 and diarrhoeal disease risk were assessed by the arithmetical health risk assessment method.
514 Results were presented in Table 5a, which depicts that children of age below 18 years old are
515 highly susceptible (viz. 39% in rainy season and 64% in winter season) for *As* ingestion
516 diseases. In Table 5b, suggests that people of age above 18 years old (i.e. female and male)
517 were found highly susceptible to hyper pigmentation and keratosis. In a total highest affected
518 population was female, in the rainy season total of 7112 (i.e. 33%) and winter season 5952 (i.e.
519 52%) female population were found susceptible to dermal effect (Table 5b). The overall results
520 of health risk assessment suggest that in a total 29,616 population of Guwahati city is at a risk

521 of *As* contaminated groundwater pollution. The fluorosis effect on the present population was
522 not found at significant risk in this health risk assessment method.

523 **4.6 3D spatial and depth wise concentration distribution**

524 Ordinary kriging method with combination of different variogram models was used to
525 understand the concentration gradient of Fe, *As*, Mn, and F^- in different depth aquifers of the
526 study area (Figure 7, 8, 9 & 10). The study area was divided into three-dimensional grid cells,
527 it is horizontally divided into 150 × 150 cells and vertically it is divided into 15 cells because
528 predominantly 15 layers were found in lithological data provided by PHED Assam. Different
529 variogram models such as gaussian, exponential and spherical were used to understand reliable
530 method results which could help to identify the safe groundwater regions in the study area.
531 High *As* and F^- contaminated regions were found along the boundary of the Khasi foothill of
532 the Meghalaya state on the south-east side of Guwahati city. Gaussian model function results
533 were found well corroborated with the measured dissolved concentration of groundwater
534 samples for Fe, *As*, Mn, and F^- in the study area. The contaminants in all aquifers were not
535 found varying in concentration, which suggests that partially homogeneous aquifer materials
536 are present in the study area (Figure 7, 8, 9 & 10). Dissolved Fe distribution in the aquifer was
537 depicting similar trends of *As* high and low concentrations which was measured in analytical
538 method, it indicates that Fe-oxy/hydroxide adsorption and desorption mechanism control the
539 *As* concentration in different depth of study area aquifers.

540 Influence of tributary river (i.e. Bharalu river) and Brahmaputra river water infiltration
541 was observed in both seasons aquifers depths (Figure 7a,b & 9a,b). Comparatively opposite
542 trends were observed between Mn and Fe concentration gradient in all aquifer depths for rainy
543 groundwater samples (Figure 7c,d, 8c,d, 9c,d & 10c,d). Distribution of F^- in the Gaussian
544 model kriging indicated that the eastern region of Guwahati city is a predominantly geogenic
545 source for the study area (Figure 6c,d, 7c,d, 8c,d and 9c,d). Concentration distribution within

546 all aquifers was observed to be similar, which suggested that vertical distribution of Fe, *As*, Mn
547 and F^- are controlled by artificial activities such as groundwater pumped out for industrial,
548 drinking and domestic purposes. Such concentration distribution variability was observed in
549 contaminant transport modelling in West Bengal (Mukherjee et al., 2007) and Assam state of
550 India (Sathe and Mahanta 2019a).

551 5 Conclusion

552 In study area, due to rapid development and increase in population, people are facing
553 shortage for safe drinking water, since last decade. The residential and commercial industries
554 are using groundwater source for daily usage. The results of hydrogeochemistry, statistical
555 analysis and minerals saturation indices for the analysed groundwater samples have deciphered
556 that the geogenic sources of *As* and F^- bearing minerals are present in the groundwater aquifers
557 of the study area. Prevalent mechanisms identified such as ion exchange, weathering (viz. that
558 of carbonate, silicate minerals), evaporation, precipitation (such as mineralization of siderite,
559 hematite, goethite, and ferrihydrite) and reductive dissolution of different minerals (viz. Fe-
560 oxy/hydroxide, fluorite, arsenolite, claudetite) in alluvial aquifers. The measured ORP values
561 during groundwater sampling with elevated Fe and *As* concentration groundwater samples
562 support the reductive dissolution mechanism of iron oxy/hydroxide minerals was the primary
563 cause for high *As* concentration in the groundwater samples.

564 The overall hydrogeochemistry of rainy and winter season data concludes that the shallow
565 depth aquifers are influenced by surface water infiltration. The identified hydrogeochemical
566 facies such as $Na^+ – Cl^-$ and $SO_4^{-2} – Ca^{+2}$ suggest that the groundwater has long residential time,
567 which allows to the Fe, *As*, F^- and Ca^{+2} bearing minerals to precipitate and interact in the
568 aquifer. Gibbs diagram revealed that the groundwater of the alluvium aquifer is susceptible to
569 dissolution mechanism of rock–water interaction and precipitation of minerals. The high

570 concentrations of Na^{+}, Ca^{+2} and HCO_3^{-} support ion exchange process to be prevailing in the
571 groundwater aquifer. Results of this study agree with the mineralization and dissolution
572 mechanism observed in minerals saturation indices found for dominant *As*, F^{-}, Fe and Mn
573 bearing minerals. The groundwater quality index results identified that majority of winter
574 season groundwater samples fall in excellent to good water category, which suggest that winter
575 groundwater is likely to be more suitable than rainy groundwater samples for drinking water
576 purposes, whereas 52% of rainy season groundwater samples were classified as unsuitable for
577 drinking water purposes. The main cause behind is depletion of groundwater table and
578 simultaneously, evaporation and adsorption of dissolved *As* and F^{-} on soil matrix. Whereas, in
579 rainy season groundwater table rises up and inducing reducing condition at shallow depth
580 aquifer, which increases dissolved concentration of *As* and F^{-} in groundwater.

581 Arithmetical health risk assessment from rainy and winter season groundwater samples
582 has predicted that children population of around 39 % and 64 % may suffer by *As* ingestion
583 risk. Furthermore, rainy and winter season groundwater samples have reviled that 4% and 2%
584 respectively, children population may suffer by an arsenical skin lesion (i.e. dermal effect). The
585 health risk assessment results have suggested that considerably high percentage of dermal
586 effect may be found in the women population than the male population in the study area.

587 Ordinary kriging method results for different depths aquifers have suggested that the
588 closely spaced contours indicates groundwater extraction rate is high from these regions. From
589 this study it can be concluded that the aquifer of depth 250 ft. to 500 ft. can be delineated as
590 safe aquifer and can be used for installation of deep tube wells for drinking water purposes.
591 Ground water quality monitoring result for this study area from year 2019 to 2020, will help
592 the public authorities to provide a pertinent and technologically viable solution to the study
593 area peoples.

Acknowledgments

This work is funded by DST and EU through the LOTUS Project No: DST/IMRCD/India EU/LOTUS/208/(G) and EU Grant No 820881. We deeply acknowledge the public health engineering department, Assam for facilitating the field sampling and sharing useful information. We thank the Department of Chemical Engineering and Department of Civil Engineering, IIT Guwahati for providing the analytical laboratory facilities.

Reference

Adimalla, N., & Venkatayogi, S. (2017). Mechanism of fluoride enrichment in groundwater of hard rock aquifers in Medak, Telangana State, South India. Environmental Earth Sciences, 76, 45. https://doi.org/10.1007/s12665-016-6362-2.

Amalraj, A., & Pius, A. 2013. Health risk from fluoride exposure of a population in selected areas of Tamil Nadu South India. Food Science and Human Wellness, 2, 75–86. https://doi.org/10.1016/J.FSHW.2013.03.005.

Apambire, W.B., Boyle, D.R., Michel, F.A., (1997). Geochemistry, genesis, and health implications of fluoriferous groundwaters in the upper regions of Ghana. Environ. Geol. 33 (1), 13 – 24. https://doi.org/10.1007/s002540050221.

Brindha, K., Rajesh, R., Murugan, R., & Elango, L. (2011). Fluoride contamination in groundwater in parts of Nalgonda district, Andhra Pradesh, India. Environmental Monitoring and Assessment, 172, 481-492.

Buchhamer, E. E., Blanes, P. S., Osicka, R. M., & Giménez, M. C. (2012). Environmental risk assessment of arsenic and fluoride in the Chaco Province, Argentina: Research advances. Journal of Toxicology and Environmental Health, Part A, 75(22-23), 1437-1450.

Bureau of Indian Standard-10500, 2012, “Indian standard drinking water specification, Second revision, pp.1-24.

619 Cerling TE, Pederson BL, Damm KLV, 1989 ”Sodium–calcium ion exchange in the
620 weathering of shales: implications for global weathering budgets. Geology 17:552–554.

621 Chauhan, A. and Singh, S., 2010 “Evaluation of Ganga water for drinking purpose by water
622 quality index at Rishikesh, Uttarakhand, India”, Report Opinion, 2(9). 53-61.

623 Chaurasia, O. P., Kumari, C., & Ankita, S. 2007 “Genotoxic effect of ground water salts rich
624 in fluoride”. Cytologia, 72(2), 141–144.

625 Chen, J., Qian, H., Wu, H., Gao, Y., & Li, X. (2017). Assessment of arsenic and fluoride
626 pollution in groundwater in Dawukou area, Northwest China, and the associated health
627 risk for inhabitants. Environmental Earth Sciences, 76(8), 314.

628 Chowdhury, R.M., Muntasir, S.Y. and Hossain, M.M., 2012 “Water quality index of water
629 bodies along Faridpur-Barisal road in Bangladesh”, Glob. Eng. Tech. Rev., 2(3). 1-8.

630 Dehbandi, R., Moore, F., & Keshavarzi, B. (2018). Geochemical sources, hydrogeochemical
631 behavior, and health risk assessment of fluoride in an endemic fluorosis area, central
632 Iran. Chemosphere, 193, 763–
633 776. https://doi.org/10.1016/J.CHEMOSPHERE.2017.11.021.

634 Edmunds, W.M., Smedley, P.L., 1996. Groundwater geochemistry and health: an overview.
635 Geol. Soc., London, Special Pub. 113 (1), 91e105

636 Enmark, G., & Nordborg, D. (2007). Arsenic in the groundwater of the Brahmaputra
637 floodplains, Assam, India–Source, distribution and release mechanisms. Minor Field
638 Study, 131, 35.

639 EPA, A. (2004). Risk Assessment Guidance for Superfund. Volume I: Human Health
640 Evaluation Manual (Part E, Supplemental Guidance for Dermal Risk Assessment) (Vol.
641 5). EPA/540/R/99.

642 Farooqi, A., 2015. Arsenic and fluoride pollution in water and soils. In: Arsenic and Fluoride
643 Contamination, pp. 1 – 16.

644 Fendorf S., Michael H. A. and van Geen A. (2010) Spatial and temporal variations of
645 groundwater arsenic in South and Southeast Asia. Science 328, 1123–1127.

646 Fisher RS, Mulican WF III (1997) “Hydrochemical evolution of sodium–sulphate and sodium–
647 chloride groundwater beneath the Northern Chihuahuan desert, Trans-Pecos, Texas,
648 USA”. Hydrogeol J 10(4):455–474.

649 Gebel, T. (2000). Confounding variables in the environmental toxicology of arsenic.
650 Toxicology, 144, 155–162.

651 Gomez, M.L., Blarasin, M.T., Martinez, D.E., (2009). Arsenic and fluoride in a loess aquifer
652 in the central area of Argentina. Environ. Geol. https://doi.org/10.1007/s00254-008-
653 1290-4.

654 Goswami, R., Rahman, M.M., Murrill, M., Sarma, K.P., Thakur, R., Chakraborti, D., (2014).
655 Arsenic in the groundwater of Majuli – The largest river island of the Brahmaputra:
656 Magnitude of occurrence and human exposure. J. Hydrol. 518 (Part C), 354–362.

657 Handa BK (1975) Geochemistry and genesis of fluoride containing groundwater in India.
658 Groundwater 13:275–281

659 Hillier, S., Inskip, H., Coggon, D., & Cooper, C. (1996). Water fluoridation and osteoporotic
660 fracture. Community Dent. Health, 13(Suppl 2), 63–68.

661 Hurtado, R., Tiemann, K.J., 2000. Fluoride occurrence in tap water at “Los Altos de Jalisco”
662 in the central Mexico region, in: Proceedings of the 2000 Conference on Hazardous
663 Waste Research. Denver, Colorado, 211–219.

664 Jiang, P., Li, G., Zhou, X., Wang, C., Qiao, Y., Liao, D., & Shi, D. (2019). Chronic fluoride
665 exposure induces neuronal apoptosis and impairs neurogenesis and synaptic plasticity:
666 role of GSK-3B/B-catenin pathway. Chemosphere, 214, 430–435.

667 Jones, S., Burt, B. A., Petersen, P. E., & Lennon, M. A. (2005). The effective use of fluorides
668 in public health. Bulletin of World Health Organization, 83, 670–
669 676. https://doi.org/10.1590/S0042-96862005000900012.

670 Kamboj N. and Kamboj V. (2019) Water quality assessment using overall index of pollution
671 in riverbed-mining area of Ganga-River Haridwar, India, Water Science, 33:1.

672 Karunanidhi, D., Aravinthasamy, P., Subramani, T., Roy, P. D., & Srinivasamoorthy, K.
673 (2019). Risk of fluoride-rich groundwater on human health: remediation through

managed aquifer recharge in a hard rock terrain, South India. Natural Resources Research, 1-27.

Khan, K., Wasserman, G.A., Liu, X., Ahmed, E., Parvez, F., Slavkovich, V., Levy, D., Mey,J., Van Geen, A., Graziano, J.H., Factor-Litvak, P., 2012. Manganese exposure from drinking water and children's academic achievement. NeuroToxic 33, 91–97.

Kumar, M., Das, A., Das, N., Goswami, R., & Singh, U. K. (2016). Co-occurrence perspective of arsenic and fluoride in the groundwater of Diphu, Assam, Northeastern India. Chemosphere, 150, 227-238.

Kumar, M., Patel, A. K., Das, A., Kumar, P., Goswami, R., Deka, P., & Das, N. (2017a). Hydrogeochemical controls on mobilization of arsenic and associated health risk in Nagaon district of the central Brahmaputra Plain, India. Environmental geochemistry and health, 39(1), 161-178.

Kumar, M., Ramanathan, A. L., Rao, M. S., & Kumar, B. (2006). Identification and evaluation of hydrogeochemical processes in the groundwater environment of Delhi, India. Environmental Geology, 50(7), 1025-1039.

Kumar, P., Singh, C. K., Saraswat, C., Mishra, B., & Sharma, T. (2017b). Evaluation of aqueous geochemistry of fluoride enriched groundwater: a case study of the Patan district, Gujarat, Western India. Water Science, 31(2), 215-229.

Mahanta, C., Sathe, S. S., & Mahagaonkar, A. (2016, June). Morphological and mineralogical evidences of arsenic release and mobilization in some large floodplain aquifers. In Arsenic research and global sustainability: Proceedings of the Sixth International Congress on Arsenic in the Environment (As2016) (p. 66).

Mahanta, Chandan, Enmark, Gustav, Nordborg, Daniel, Sracek, Ondra, Nath, Bibhash, Nickson Ross, T., Herbert, Roger, et al., 2015. Hydrogeochemical controls on mobilization of arsenic in groundwater of a part of Brahmaputra river floodplain, India. J. Hydrol. Reg. Stud. 4, 154 – 171.

Mandal B.K., Suzuki K.T., 2002 "Arsenic round the world: a review", Talanta 58; 201–235.

Mridha, D., Priyadarshni, P., Bhaskar, K., Gaurav, A., De, A., Das, A., ... & Roychowdhury, T. (2021). Fluoride exposure and its potential health risk assessment in drinking water and staple food in the population from fluoride endemic regions of Bihar, India. Groundwater for Sustainable Development, 13, 100558.

Mukherjee, A., Fryar, A., Howell, P., (2007). Regional hydrostratigraphy and groundwater flow modeling in the arsenic-affected areas of the western Bengal basin, West Bengal, India. Hydrogeol. J. 15 (7), 1397 – 1418.

Mukherjee, A., Saha, D., Harvey, C. F., Taylor, R. G., Ahmed, K. M., & Bhanja, S. N. (2015). Groundwater systems of the Indian sub-continent. Journal of Hydrology: Regional Studies, 4, 1-14.

Nakazawa, K., Nagafuchi, O., Otede, U., Chen, J. Q., Kanefuji, K., & Shinozuka, K. I. (2020). Risk assessment of fluoride and arsenic in groundwater and a scenario analysis for reducing exposure in Inner Mongolia. RSC Advances, 10(31), 18296-18304.

National Research Council (1999). Arsenic in drinking water. National Academies Press. Washington, DC.

Njuguna, S.M., Anyango, V., Yan, X., Wahiti, R.W., Wang, Q., Wang, J., 2019. Healthrisk assessment by consumption of vegetables irrigated with reclaimed wastewater: a case study in Thika (Kenya). J. Environ. Manage. 231, 576–581.

Nordstrom D.K.,2002 “Public health: enhanced: worldwide occurrences ofarsenic in ground water,” Science 296; 2143–2145.

Oliver, M. A., & Webster, R. (1990). Kriging: a method of interpolation for geographical information systems. International Journal of Geographical Information System, 4(3), 313-332.

Patel, A. K., Das, N., Goswami, R., & Kumar, M. (2019). Arsenic mobility and potential co-leaching of fluoride from the sediments of three tributaries of the Upper Brahmaputra floodplain, Lakhimpur, Assam, India. Journal of Geochemical Exploration, 203, 45-58.

Patel, Khageshwar Singh, Bharat Lal Sahu, Nohar Singh Dahariya, Amarpreet Bhatia, Raj Kishore Patel, Laurent Matini, Ondra Sracek, and Prosun Bhattacharya. 2017

729 "Groundwater arsenic and fluoride in Rajnandgaon District, Chhattisgarh, northeastern
730 India." Applied Water Science 7, no. 4: 1817-1826.

731 Petersen, P. E., & Lennon, M. A. (2004). Effective use of fluorides for the prevention of dental
732 caries in the 21st century: the WHO approach. Community Dentistry and Oral
733 Epidemiology, 32, 319–321. https://doi.org/10.1111/j.1600-0528.2004.00175.x.

734 Piper AM (1944) A graphical interpretation of water—analysis. Trans Am Geophys Union
735 25:914–928.

736 Podgorny, P. C., & McLaren, L. (2015). Public perceptions and scientific evidence for
737 perceived harms/risks of community water fluoridation: an examination of online
738 comments pertaining to fluoridation cessation in Calgary in 2011. Canadian Journal of
739 Public Health, 106, 413–425. https://doi.org/10.17269/CJPH.106.5031.

740 Population of Guwahati 2020 (Demographic, Facts, Etc) – India Population 2020".

741 Rasool, A., Xiao, T., Baig, Z. T., Masood, S., Mostofa, K. M., & Iqbal, M. (2015). Co-
742 occurrence of arsenic and fluoride in the groundwater of Punjab, Pakistan: source
743 discrimination and health risk assessment. Environmental Science and Pollution
744 Research, 22(24), 19729-19746.

745 Rown, R.M, McCleiland, N.J., Deiniger, R.A. and O'Connor, M.F.A. 1972 "Water quality
746 index – crossing the physical barrier", (Jenkis, S.H. ed.) Proceedings in International
747 Conference on water pollution Research Jerusalem 6. 787-797.

748 Saleem, M., Iqbal, J., Shah, M.H., 2019. Seasonal variations, risk assessment and multivariate
749 analysis of trace metals in the freshwater reservoirs of Pakistan. Chemo 216, 715–724.

750 Sathe, S. S. 2019b. Study to delineate arsenic safe and unsafe aquifers by hydrogeological,
751 microbiological and numerical methods (Doctoral dissertation).

752 Sathe, S. S., and Mahanta, C. 2019a. Groundwater flow and arsenic contamination transport
753 modeling for a multi aquifer terrain: Assessment and mitigation strategies. Journal of
754 environmental management, 231, 166-181.

Sathe, S. S., Goswami, L., Mahanta, C., & Devi, L. M. 2020. Integrated factors controlling arsenic mobilization in an alluvial floodplain. Environmental Technology & Innovation, 17, 100525.

Sathe, S. S., Mahanta, C., & Mishra, P. (2018). Simultaneous influence of indigenous microorganism along with abiotic factors controlling arsenic mobilization in Brahmaputra floodplain, India. Journal of contaminant hydrology, 213, 1-14.

Sathe, S., Mahanta, C., Mahagaonkar, A., 2016. Evidence of Microbiological Control of Arsenic Release and Mobilization in Aquifers of Brahmaputra Flood Plain, Arsenic Research and Global Sustainability: Proceedings of the Sixth International Congress on Arsenic in the Environment (As2016), June 19–23, 2016. CRC Press, Stockholm, Sweden, pp. 115.

Saxena VK, Ahmed S (2003) Inferring the chemical parameters for the dissolution of fluoride in groundwater. Environ Geol 43:731–736

Schaefer, Michael V., Xinxin Guo, Yiqun Gan, Shawn G. Benner, Aron M. Griffin, Christopher A. Gorski, Yanxin Wang, and Scott Fendorf. 2017 "Redox controls on arsenic enrichment and release from aquifer sediments in central Yangtze River Basin." Geochimica et Cosmochimica Acta 204: 104-119.

Schuh WM, Klinekebiel DL, Gardner JC, Meyar RF, 1997. Tracer and nitrate movements to groundwater in the Norruem Great Plains. J Environ Qual 26:1335–1347

Singh, A.K. 2004, Arsenic contamination in the groundwater of North Eastern India Proceedings on National Seminar on Hydrology, Roorkee, Nov 22–24 (2004)

Singh, S. K., & Ghosh, A. K. (2012). Health risk assessment due to groundwater arsenic contamination: Children are at high risk. Human and Ecological Risk Assessment, 18, 751–766.

Smedley, P. L., & Kinniburgh, D. G. (2002). A review of the source, behavior and distribution of arsenic in natural waters. Applied Geochemistry, 17(5), 517–568.

Srinivasa Rao, N. (1997). The occurrence and behaviour of fluoride in the groundwater of the Lower Vamsadhara River basin, India. Hydrological Sciences, 42(6), 877-892.

Sun, L., Gao, Y., Liu, H., Zhang, W., Ding, Y., Li, B., Li, M., & Sun, D. (2013). An assessment of the relationship between excess fluoride intake from drinking water and essential hypertension in adults residing in fluoride endemic areas. Science of the Total Environment, 443, 864–869. https://doi. org/10.1016/J.SCITOTENV.2012.11.021.

Susheela, A., Bhatnagar, M., Vig, K., & Mondal, N. (2005). Excess fluoride ingestion and thyroid hormone derangements in children living in Delhi, India. Fluoride, 38, 98–108 ISSN 0015–4725.

USEPA, 2004. Risk Assessment Guidance for Superfund: Human Health EvaluationManual (Part E).

Valdez-Jiménez, L., Soria Fregozo, C., Miranda Beltrán, M.L., Gutiérrez Coronado, O., Pérez Vega, M.I., 2011. Effects of the fluoride on the central nervous system. Neurology, (English Ed. 26, 297–300. https://doi.org/10.1016/S2173- 5808(11)70062-1.

Vaiphei, S. P., & Kurakalva, R. M. (2021). Hydrochemical characteristics and nitrate health risk assessment of groundwater through seasonal variations from an intensive agricultural region of upper Krishna River basin, Telangana, India. Ecotoxicology and Environmental Safety, 213, 112073.

van Geen, A., et al., 2008a. Comparison of arsenic concentrations in simultaneously collected groundwater and aquifer particles from Bangladesh, India, Vietnam, and Nepal. Appl. Geochem. 23 (11), 3244–3251.

van Geen, A., et al., 2008b. Flushing history as a hydrogeological control on the regional distribution of arsenic in shallow groundwater of the Bengal Basin. Environ. Sci. Technol. 42 (7), 2283–2288.

Wen, D., Zhang, F., Zhang, E., Wang, C., Han, S., & Zheng, Y. (2013). Arsenic, fluoride and iodine in groundwater of China. Journal of Geochemical Exploration, 135, 1-21.

Wenzel, W. W., & Blum, W. E. (1992). Fluorine speciation and mobility in F-contaminated soils. Soil Science, 153(5), 357-364.

WHO. (1993). Guidelines for drinking-water quality (2nd ed., Vol. 1).

Xiong, X., Liu, J., He, W., Xia, T., He, P., Chen, X., Yang, K., & Wang, A. (2007). Dose–effect relationship between drinking water fluoride levels and damage to liver and kidney functions in children. Environmental Research, 103(1), 112–116. https://doi.org/10.1016/j.envres.2006.05.008.

Yadav, K. K., Kumar, S., Pham, Q. B., Gupta, N., et al. (2019). Fluoride contamination, health problems and remediation methods in Asian groundwater: a comprehensive review. Ecotoxicology and Environmental Safety, 182, 109362.

Figures

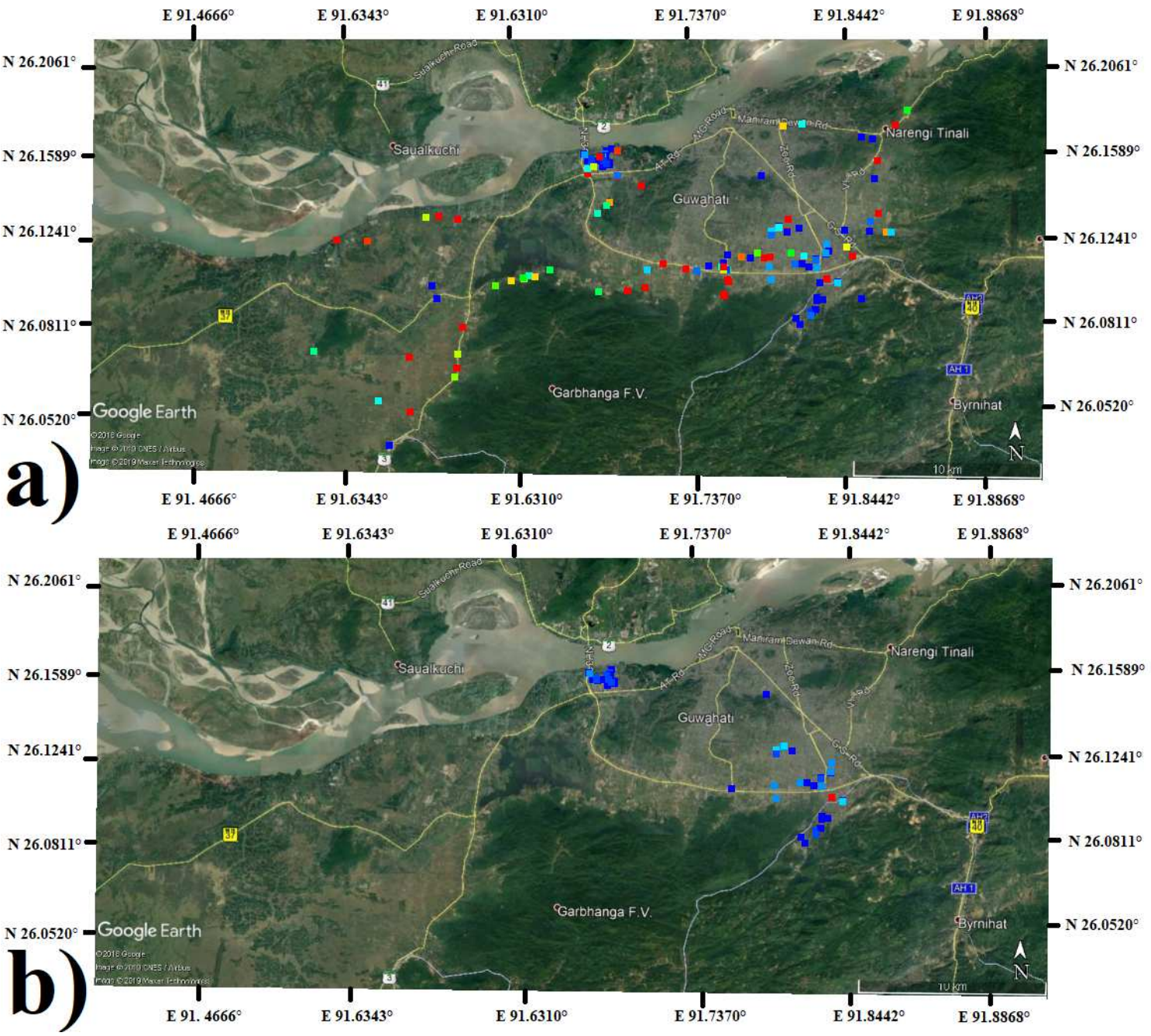

Figure 1

Study area map shows groundwater sampling location of a) Rainy season (n=94) and b) Winter season (n=50) in Guwahati city. Note: The designations employed and the presentation of the material on this map do not imply the expression of any opinion whatsoever on the part of Research Square concerning the legal status of any country, territory, city or area or of its authorities, or concerning the delimitation of its frontiers or boundaries. This map has been provided by the authors.

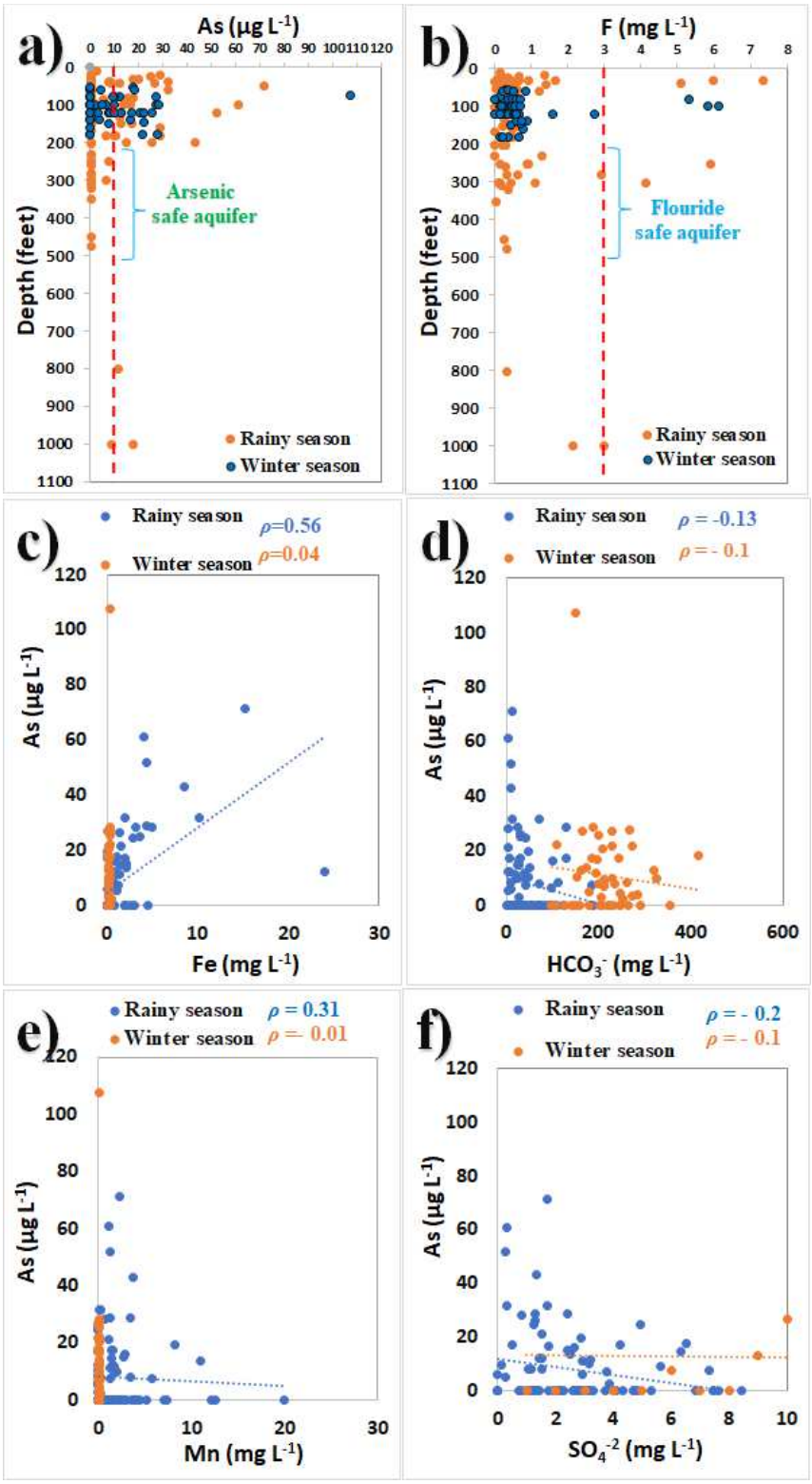

Figure 2

a) and b) distribution of dissolved arsenic and fluoride concentration in shallow and deeper aquifer, Scatter plot showed Pearson correlation between c) As vs Fe d) As vs HCO3– e) As vs Mn and f) As vs SO4–2

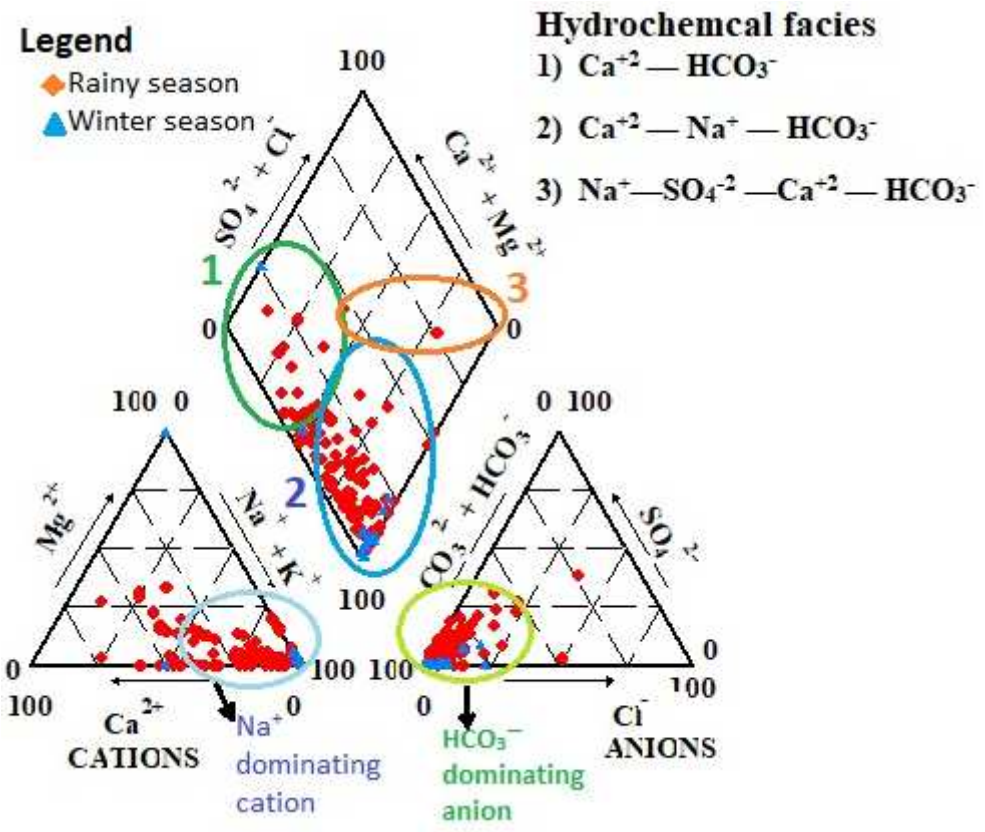

Figure 3

Piper plot showed predominate groundwater facies present in the rainy and winter season groundwater samples of Guwahati city

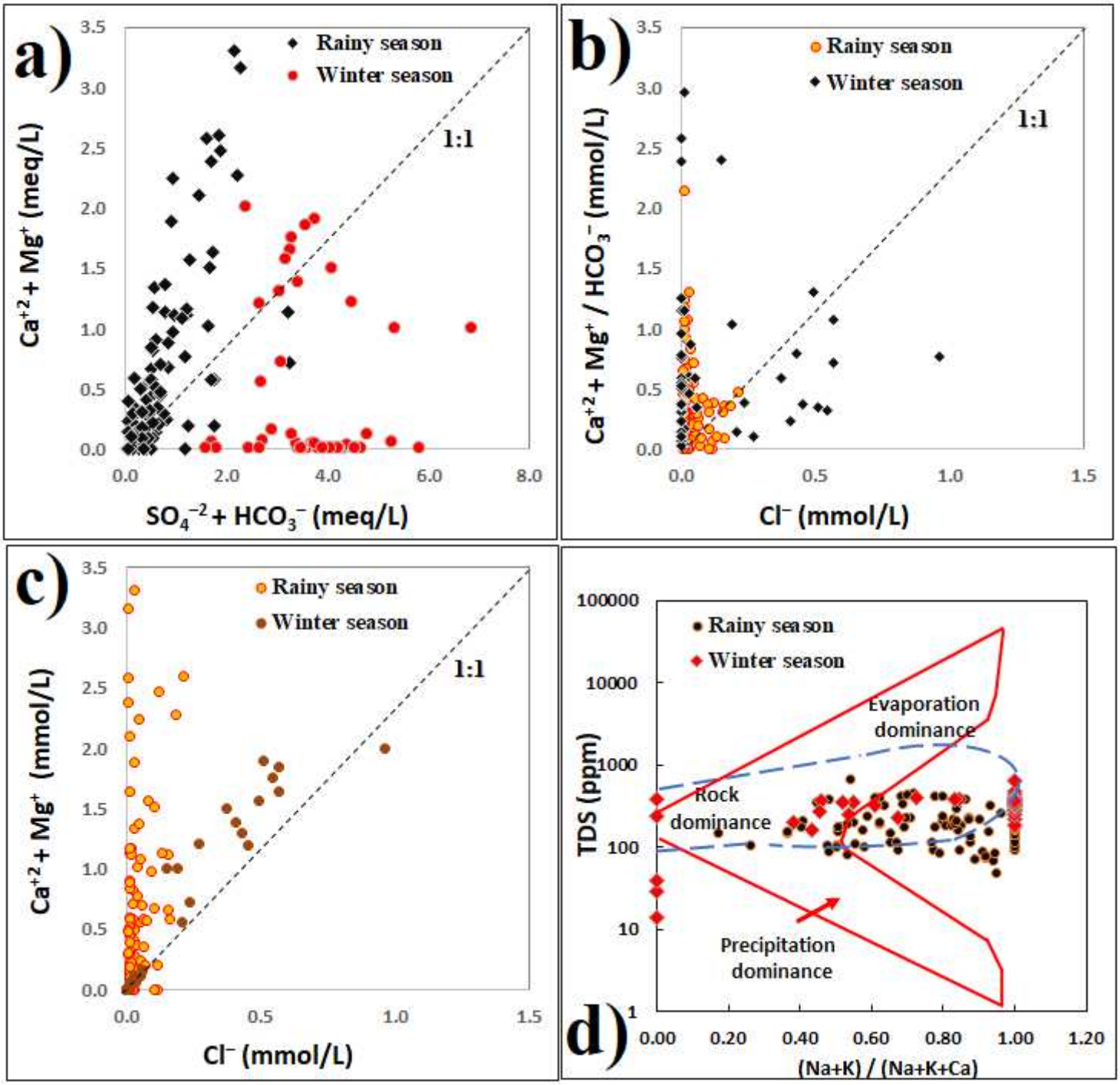

Figure 4

Scatter plot showed relation between dissolved cation and anion in a), b), c) and d) Gibbs plot for rainy and winter season groundwater samples

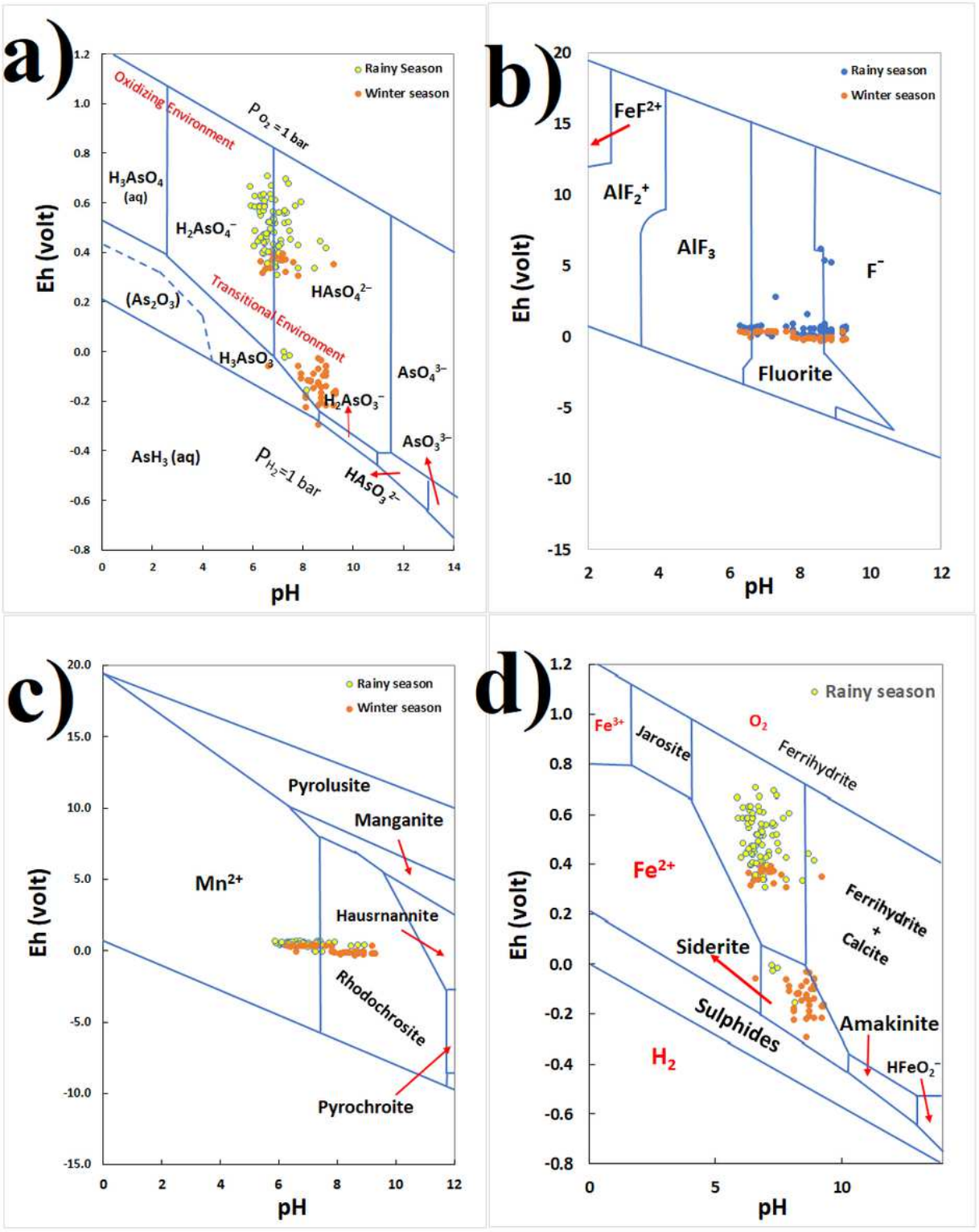

Figure 5

Pourbaix diagram showed species of a) arsenic b) fluoride c) manganese and d) iron in the groundwater aquifer.

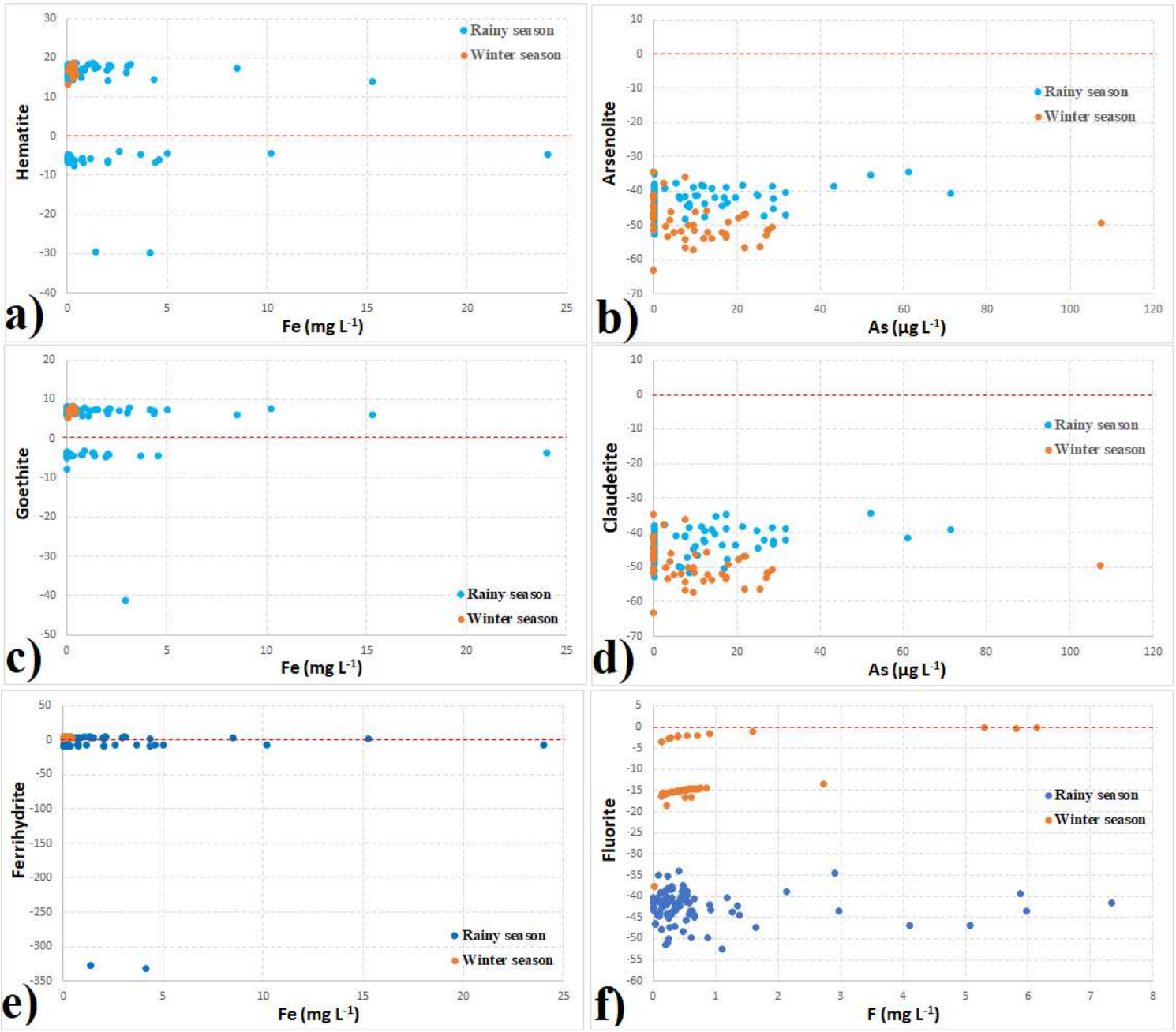

Figure 6

Bivariate plots showed variation of minerals saturation profile with two season dissolved concentration of iron, arsenic and fluoride in groundwater samples of Guwahati city for a) hematite b) arsenolite c) goethite d) claudetite e) ferrihydrite and f) fluorite minerals

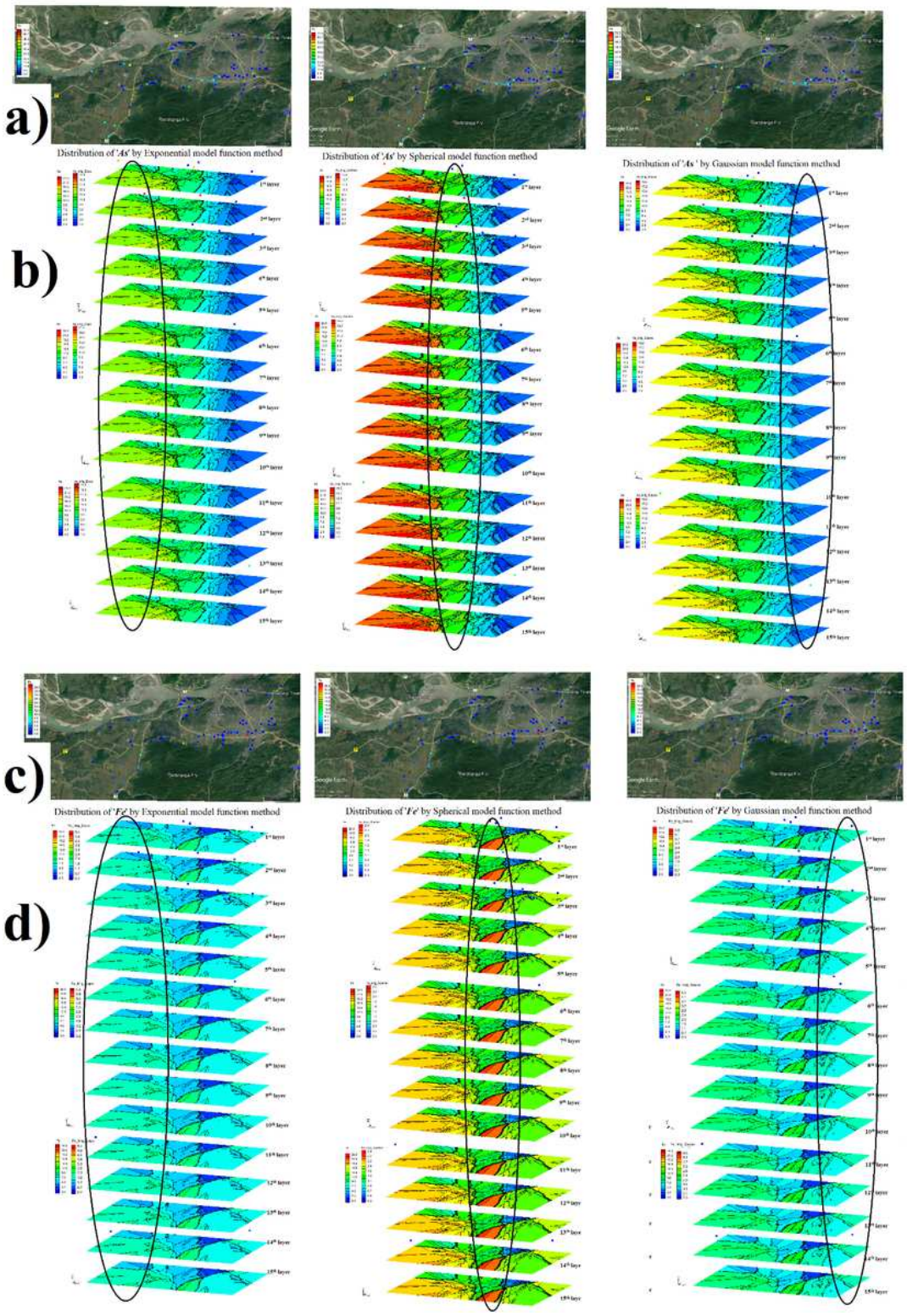

Figure 7

Kriging method showed spatial and depth wise concentration distribution of rainy season groundwater sample for arsenic in a) & b) and iron in c) & d) 3D map. Note: The designations employed and the presentation of the material on this map do not imply the expression of any opinion whatsoever on the part of Research Square concerning the legal status of any country, territory, city or area or of its

authorities, or concerning the delimitation of its frontiers or boundaries. This map has been provided by the authors.

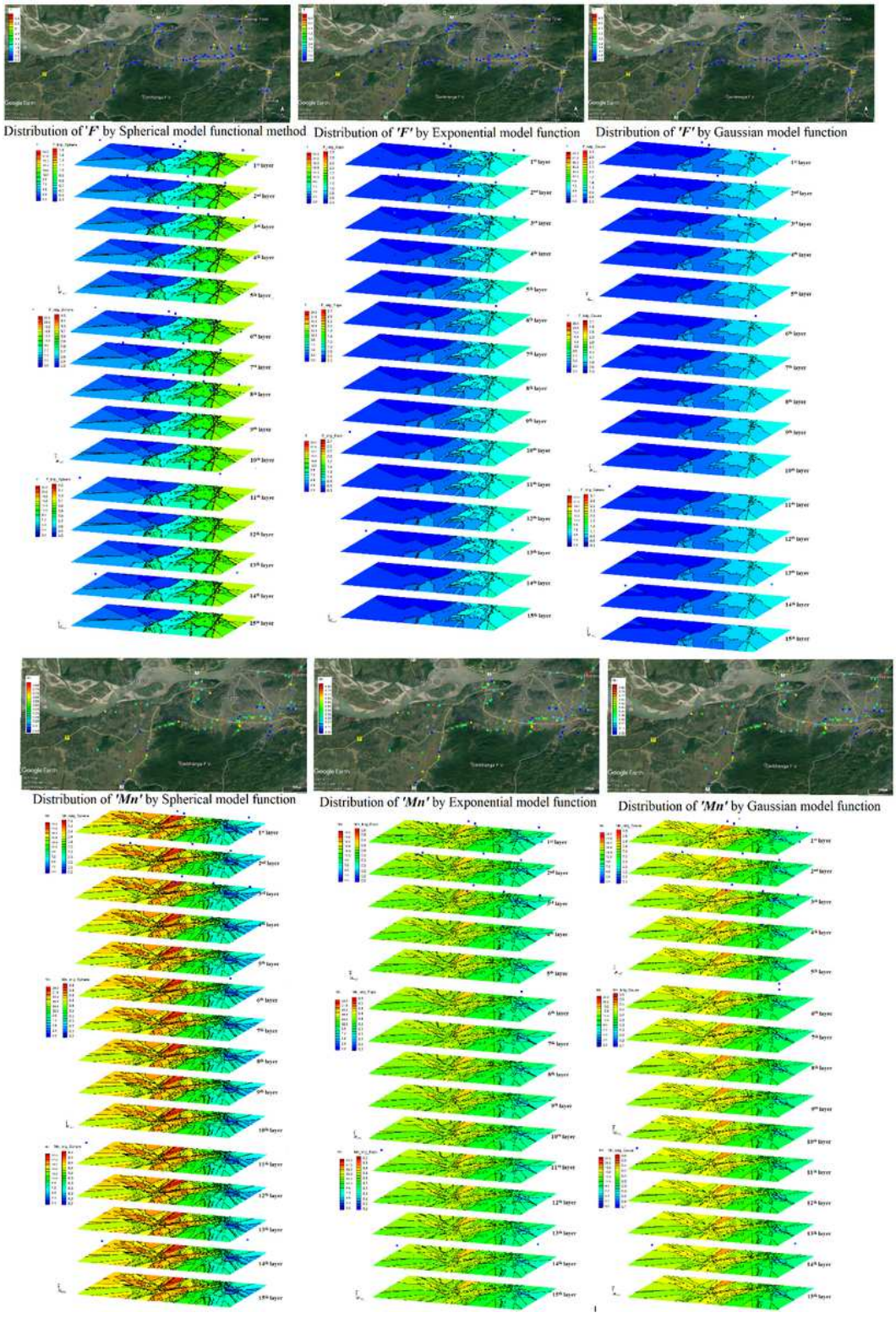

Figure 8

Kriging method showed spatial and depth wise concentration distribution of rainy season groundwater sample for fluoride in a) & b) and manganese in c) & d) 3D map. Note: The designations employed and the presentation of the material on this map do not imply the expression of any opinion whatsoever on

the part of Research Square concerning the legal status of any country, territory, city or area or of its authorities, or concerning the delimitation of its frontiers or boundaries. This map has been provided by the authors.

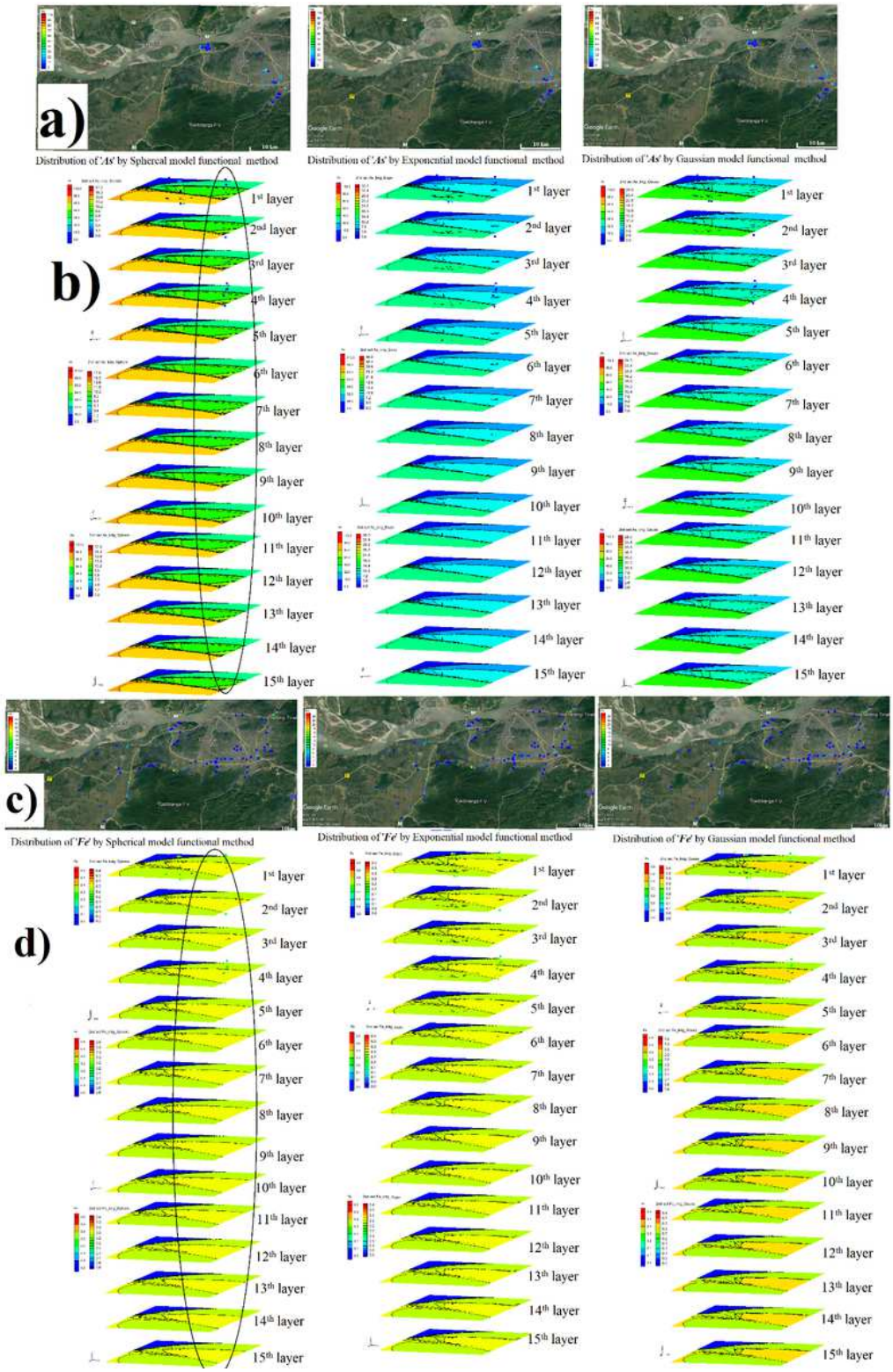

Figure 9

Kriging method showed spatial and depth wise concentration distribution of winter season groundwater sample for arsenic in a) & b) and iron in c) & d) 3D map. Note: The designations employed and the

presentation of the material on this map do not imply the expression of any opinion whatsoever on the part of Research Square concerning the legal status of any country, territory, city or area or of its authorities, or concerning the delimitation of its frontiers or boundaries. This map has been provided by the authors.

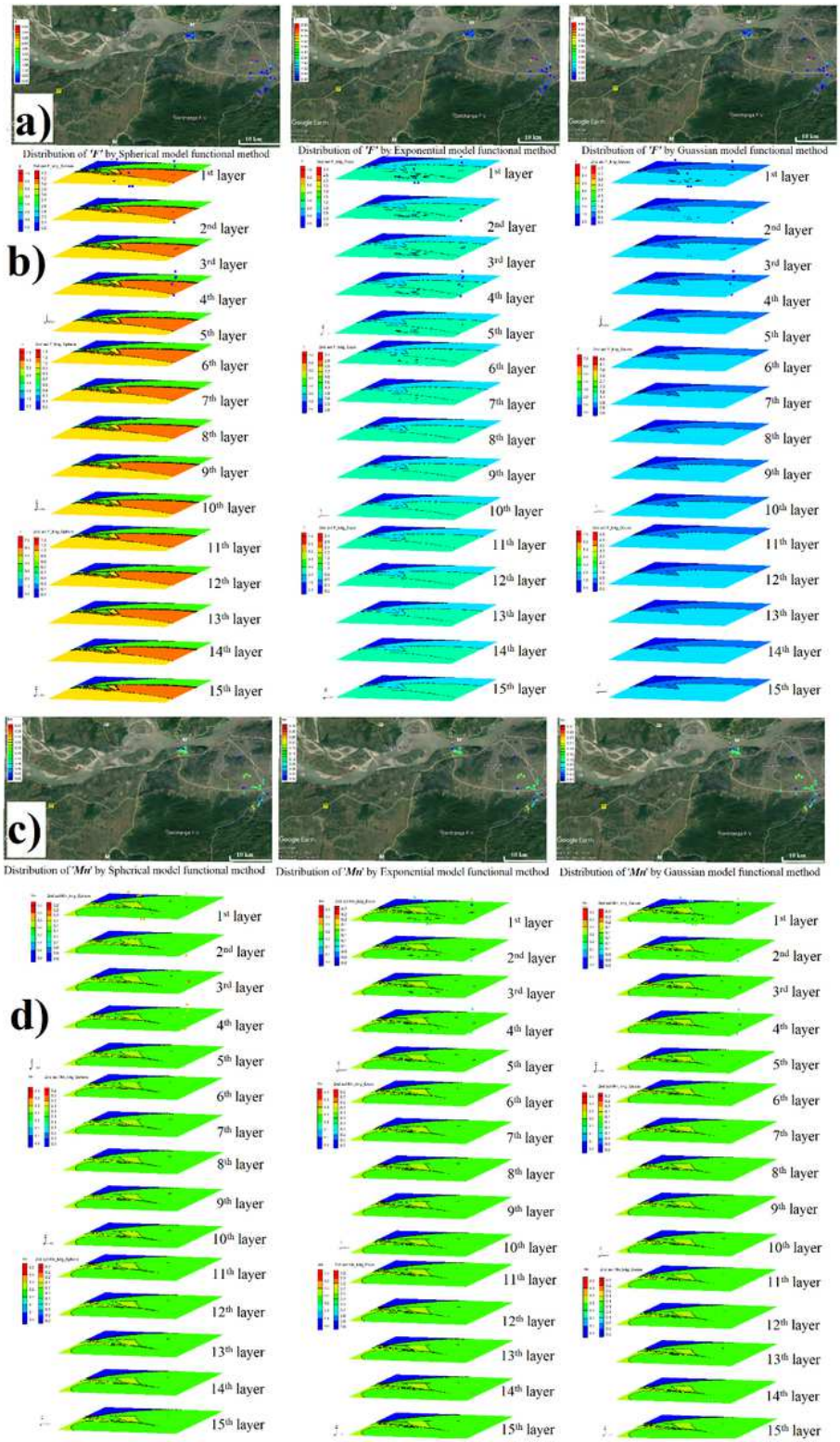

Figure 10

Kriging method showed spatial and depth wise concentration distribution of winter season groundwater sample for fluoride in a) & b) and manganese in c) & d) 3D map. Note: The designations employed and the presentation of the material on this map do not imply the expression of any opinion whatsoever on the part of Research Square concerning the legal status of any country, territory, city or area or of its authorities, or concerning the delimitation of its frontiers or boundaries. This map has been provided by the authors.